Thus, the initiating step never occurs in conditions where no methanesulfonic acid is formed by hydrolysis of the trimethylsilyl ester.

The fact that the oxacycle 1,3-dioxepane works better than the electron-rich styrenes might be traced to the greater affinity of Si toward O rather than toward C. Note that all the organic chemistry of trimethylsilyl triflate involves oxygen compounds, ketones and acetate, but not vinyls even if they are very electron rich.[8] So our polymer chemistry results are in accord with the known organic chemistry of these compounds. However, even in the successful case of 1,3-dioxepane with trimethylsilyl methanesulfonate, the initiation step is slow relative to propagation as shown by the long reaction times, high molecular weights, and broad molecular distributions.

Experimental Section

Methods. ^{1}H NMR spectra were recorded on a Brucker WM-250 spectrometer. Deuteriochloroform and dichlorodimethylsilane were used as the solvent and internal reference. Molecular weights of polymers were measured on a Shodex GPC A 804 column calibrated with polystyrene and THF standards, chloroform as eluent, and a Waters RI detector. Elemental analyses were performed by Desert Analytics, Tucson, AZ.

Monomers. *p*-Methoxystyrene, anethole, 1,3-dioxolane, and trioxane were purchased from Aldrich and purified by distillation over calcium hydride under reduced pressure. 1,3-Dioxepane was made from 1,4-butanediol and paraformaldehyde according to the method of Astle et al.[9] 4-Isopropenylanisole was made from 4-bromoanisole and acetone in the presence of magnesium.

Initiators. Trimethylsilyl diphenyl phosphate was made from the reaction of excess trimethylsilyl chloride with silver diphenylphosphate in acetonitrile in the dark at room temperature. After the silver chloride is filtered off, the solvent is evaporated and the viscous residue distilled (bp 119 °C (0.2 torr)). Yield 90%. Trimethylsilyl methanesulfonate was purchased from Aldrich.

Polymerization. A glass vessel with two arms containing small magnetic stirrers and an NMR tube were heated under 0.05 mmHg, until the magnets inside the stirrers could be seen (about 400 °C). The tube was then filled with argon and placed inside a glovebag. While argon was continuously purged into the tube, monomer, initiator, $CDCl_3$, and 2,6-di-*tert*-butyl-4-methylpyridine, which had been carefully purified, were put into the different arms: monomer, $CDCl_3$, and CaH_2 in one arm; initiator, hindered base, and $CDCl_3$ in the other one. The tube was closed and the contents stirred for about 20 h (argon was still continuously purged). The NMR tube was reheated to about 400 °C under 0.05 mmHg while the contents of the arms were cooled in liquid nitrogen. Under full vacuum (<0.05 mmHg) the NMR tube was cooled by liquid nitrogen and monomer, initiator, and $CDCl_3$ were distilled very carefully into the NMR tube, which was then sealed off.

Acknowledgment. We thank the S. C. Johnson Co. and the E. I. du Pont de Nemours and Co. for financial support and a Referee for extremely helpful comments. Acknowledgment is made to the donors of the Petroleum Research Fund, administered by the American Chemical Society, for partial support of this work.

References and Notes

(1) Gandini, A.; Cheradame, H. *Encycl. Polym. Technol. Second Ed.* **1986**, *2*, 729.
(2) Chiatowska, W.; Kubisa, P.; Penczek, S. *Makromol. Chem.* **1982**, *183*, 753.
(3) Hwu, J. R.; Wetzel, J. M. *J. Org. Chem.* **1985**, *50*, 3946.
(4) Gong, M. S.; Hall, H. K., Jr. *Macromolecules* **1987**, *19*, 3011.
(5) Sawamoto, M.; Kamigatio, M.; Kujima, K.; Higashimura, T. *Polym. Bull.* **1988**, *19*, 359.
(6) Collomb, J.; Arland, P.; Gandini, A.; Cheradame, H. In *Cationic Polymerization and Related Processes*; Goethals, E. J., Ed.; Academic Press: New York, 1984, p 49.
(7) Gandini, A.; Martinez, A. *Makromol. Chem.-Macromol. Symp.* **1988**, *13/14*, 211.
(8) Noyori, R.; Murata, S.; Suzuki, M. *Tetrahedron* **1981**, 3899.
(9) Astle, M.; Zaslowski, J. A.; Lofyatis, P. G. *Ind. Eng. Chem.* **1954**, *46*, 787.

Registry No. Trimethylsilyl diphenylphospate, 25723-74-4; *p*-methoxystyrene, 637-69-4; anethole, 104-46-1; 4-isopropenylanisole, 1712-69-2; 2,6-di-*tert*-butylpyridine, 585-48-8; trimethylsilyl methanesulfonate, 10090-05-8; allyl-*tert*-butyldimethylsilane, 74472-22-3; triflic acid, 1493-13-6; *tert*-butyldimethylsilane, triflate, 69739-34-0; (*tert*-butyldimethylsilyl)methanesulfonate, 124156-70-3; 1,3-dioxepane, 505-65-7; 1,3-dioxepane (homopolymer), 25037-55-2; 1,3-dioxolane, 646-06-0; trioxane, 110-88-3; methanesulfonic acid, 75-75-2.

Modeling of the Epitaxial Crystallization of Poly(vinylidene fluoride): T_2, TGTG′, and T_3GT_3G' Chain Conformations on (111) CaF_2

R. E. MORTON

Westinghouse Electric Corporation, Measurements and Control Division, Raleigh, North Carolina 27604

C. M. BALIK*

Department of Materials Science and Engineering, Box 7907, North Carolina State University, Raleigh, North Carolina 27695. *Received June 16, 1989; Revised Manuscript Received August 3, 1989*

Introduction

In an earlier paper,[1] the epitaxial deposition of poly(vinylidene fluoride) (PVF_2) on a (111) CaF_2 substrate was modeled using molecular mechanics. A single PVF_2 chain segment consisting of 10 repeat units frozen into the all-trans (T_2) conformation was used to represent the polymer. It was found that the Coulombic contribution to the total polymer–substrate interaction energy was quite high (about 40%) as compared with other polymer epitaxial systems that have been modeled using this method. The orientation resulting in the lowest energy was one in which the plane of the planar zigzag backbone of the PVF_2 chain was parallel to the substrate and centered over a row of fluoride ions. The total interaction energy for this orientation was −55.4 kcal mol^{-1}/10 PVF_2 repeat units. The CF_2 dipoles in this orientation are parallel to the substrate. Another low-energy orientation (E_{min} = −53.4 kcal mol^{-1}/10 PVF_2 repeat units) was also found in which the CF_2 dipoles were normal to the substrate surface, with the polymer fluorine atoms next to the surface. Boltzmann statistics predicted that approximately 14% of the PVF_2 chain segments should deposit in the latter orientation. The other known chain conformations of PVF_2, TGTG′, and T_3GT_3G' were not considered. The purpose of this note is to summarize the results of these calculations for the last two chain conformations and to compare them with those of the T_2 conformation.

Theory and Methods

Details of the interaction energy calculations have been described in the earlier work and will only be summa-

0024-9297/90/2223-0680$02.50/0

Table I
Lowest Energy Minima Found for the Three PVF_2 Chain Conformations on (111) CaF_2

conformn	x, Å	y, Å	h, Å	ϕ, deg	μ, deg	energy[a]	% Coulombic	P_i
T_2	0.6	2.6	1.4	0	280	−70.1	47.8	0.81
T_2	0.6	0.6	1.4	0	80	−68.8	46.5	0.19
TGTG′	0.0	0.0	1.4	106	10	−45.8	43.4	0.35
TGTG′	0.0	2.1	1.3	0	245	−45.6	32.2	0.29
TGTG′	0.0	1.2	1.3	0	115	−45.3	31.1	0.22
T_3GT_3G'	0.0	0.0	1.2	97	30	−37.9	31.4	0.50
T_3GT_3G'	0.0	0.0	1.2	37	30	−37.7	30.5	0.40

[a] Units = kcal mol^{-1}/10 PVF_2 repeat units.

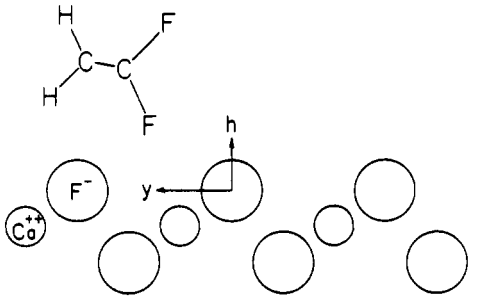

Figure 1. Schematic end-view projection showing the PVF_2T_2 conformation in the lowest energy orientation with (x, y, h, ϕ, μ) = (0.6 Å, 2.6 Å, 1.4 Å, 0°, 280°).

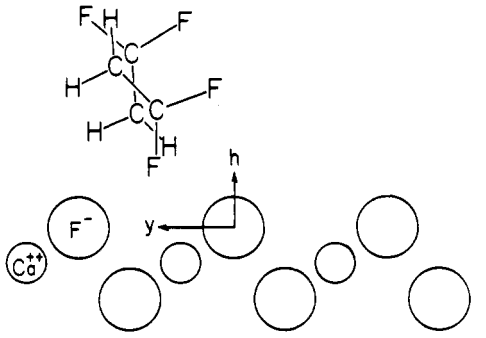

Figure 2. Schematic end-view projection showing the PVF_2TGTG' conformation in a low-energy orientation with (x, y, h, ϕ, μ) = (0 Å, 2.1 Å, 1.3 Å, 0°, 245°).

rized briefly here. The total interaction energy is the sum of all pairwise polymer atom–substrate ion interactions. Both coulombic and dispersion–repulsive (6–12) potentials were included. Five spatial variables describe the orientation of the polymer segment with respect to the substrate. The position of a point at the end of the chain segment and on the chain axis is given by (x, y), where x and y represent translations from the origin (a fluoride ion) on the substrate surface. The height above the substrate, h, was measured from the polymer atom(s) closest to the surface. The rotation about the polymer chain axis is given by μ, with μ = 0 corresponding to CF_2 dipole orientation normal to the surface, with the fluorine atoms next to the surface. The rotation of the polymer chain axis about a normal to the surface is given by ϕ, with ϕ = 0 corresponding to the substrate ⟨$\bar{1}$10⟩ directions (parallel to and centered over a row of fluoride ions). In the earlier work, only three values of μ were considered: μ = 0, 90, and 180°. In the present work, μ was explored from 0 to 360° at 5° intervals. When these additional μ rotations were applied to the T_2 conformation, the positions of the energy minima changed slightly, and the minimum energy was significantly lowered. These refinements to the T_2 conformation have been reported here. The increments used for the other variables were 0.1 Å for x, y, and h and 1° for ϕ. The polymer chain axis was maintained parallel to the substrate in all cases.

The polymer segments used for the T_2 and TGTG′ conformations contained 10 PVF_2 repeat units. In order to provide an integral number of fiber repeats, the segment used for the T_3GT_3G' conformation contained 12 repeat units. Bond lengths and bond angles for the TGTG′ conformation were taken from the crystal structure data of Bachmann et al.[2] and for the T_3GT_3G' conformation from Weinhold et al.[3] Potential parameters have been listed in the earlier paper.

Results and Discussion

Isoenergy contour plots involving different pairs of the independent spatial variables were constructed and analyzed for each chain conformation. The lowest energy minima found for each of the three PVF_2 chain conformations are listed in Table I. For the T_2 conformation, the two minima listed were the only ones located with energies near −70 kcal mol^{-1}/10 repeat units. A total of 14 minima with energies ranging from −37.4 to −45.8 kcal mol^{-1}/10 repeat units were found for the TGTG′ conformation, and 17 minima were found for the T_3GT_3G' conformation, with energies ranging from −31.7 to −37.9 kcal mol^{-1}/10 repeat units. Boltzmann statistics were applied to estimate the fraction of PVF_2 chain segments that would occupy each energy minimum for each conformation. The probability of finding a chain segment in a particular energy minimum is given by

$$P_i = \frac{\exp(-E_i/RT)}{\sum_i \exp(-E_i/RT)} \quad (1)$$

where E_i is the minimum interaction energy, T = 170 °C, and the sum is taken over all low-energy minima for each chain conformation (2 for the T_2, 14 for the TGTG′, and 17 for the T_3GT_3G' conformation). These values have been listed in the last column of Table I. From this estimate, at least 86% of the epitaxially deposited PVF_2 chain segments in each conformation are accounted for by the minima listed in Table I. These numbers also indicate that the population of low-energy states is fairly evenly split for the TGTG′ and T_3GT_3G' conformations, while the minimum associated with μ = 280° for the T_2 conformation is strongly preferred over the other minimum at μ = 80°.

The deepest and most distinct energy minima were found for the T_2 conformation. The minimum energies found at μ = 80 and 280° are at least 13 kcal mol^{-1}/10 repeat units lower than those reported in the earlier work, in which μ was limited to only three values. These single-chain interaction energy calculations therefore predict that the T_2 conformation is energetically favored to epitaxially deposit on a (111) CaF_2 surface. This is pri-

marily due to the larger contribution of the coulombic interaction energy, as the absolute values of the dispersion–repulsive energies are quite similar for all three conformations. The "smoother" nature of the surface of the polymer chain in the TGTG′ and the T_3GT_3G' conformations results in a smoother and less distinct interaction energy hypersurface, which contains several minima having similar energies. In all cases, the coulombic contribution to the total interaction energy is relatively high, although the effect of the coulombic potential on the contour plots was much less pronounced for the T_3GT_3G' conformation as compared with the other two. This reflects the less polar nature of the T_3GT_3G' conformation.

A careful consideration of the polymer–substrate orientational relationships that exist at each energy minimum revealed that polymer fluorine atoms tend to align close to a row of Ca^{2+} ions in the substrate (0.78 Å below the surface layer of F^- ions). This is the source of the large coulombic interaction and seems to be the determining factor in the location of several of the energy minima listed in Table I. Representative examples are shown in the schematic end-view projections in Figures 1 and 2 for the T_2 and TGTG′ conformations, respectively. An end-view projection for the T_3GT_3G' conformation in one of its low-energy minima is not shown because the ϕ angles at which they occur are not integer multiples of 60°, which renders the projection of the substrate atoms cluttered and uninformative.

Identical energy minima were found at 120° intervals of ϕ (other parameters constant) for all three conformations, reflecting the trigonal symmetry of the of the (111) CaF_2 surface. Within each 120° interval, several additional minima having nearly equal energies were also noted, especially for the TGTG′ and T_3GT_3G' conformations. The particular ϕ angles at which any of these minima occur could be justified by comparing the polymer fiber repeat distance with the substrate repeat distance along each ϕ direction. In each case, an energy minimum occurs when the characteristic spacing between substrate ions and the polymer fiber repeat form a low-order "lattice match".

Of particular interest in this work are the CF_2 dipole orientations in the energy minima and the potential for epitaxially producing a spontaneously piezoelectric film of PVF_2. Only the component of the dipole moment that is normal to the surface will contribute, since the components parallel to the surface will average out as a result of the equal probability of PVF_2 chains aligning in three equally spaced directions on the surface. The component of the dipole moment normal to the surface for one PVF_2 chain segment, located in the ith energy minimum and having chain conformation j, is given by $\epsilon_j \cos \mu_i$, where ϵ_j is the magnitude of the dipole moment for chain conformation j. The net dipole moment for a bulk epitaxial film of PVF_2 having chain conformation j, ϵ_j(net), was estimated using the following equation

$$\epsilon_j(\text{net}) = \epsilon_j \sum_i P_i \cos \mu_i \qquad (2)$$

where the sum is over the low-energy minima for chain conformation j. All low-energy minima were included in this sum for each conformation, not just those listed in Table I, even though the additional minima make a minor contribution to the final result. Results of these calculations are listed in Table II. Dipole moments are given in units of debye/PVF_2 repeat unit.

Table II
Predicted Net Dipole Moments for Epitaxial Films of PVF_2 on (111) CaF_2

conformn	ϵ_j[a]	$\sum_i P_i \times \cos \mu_i$	ϵ_j(net)[a]
T_2	2.1[b]	0.17	0.36
TGTG′	1.3[b]	0.08	0.10
T_3GT_3G'	1.1[c]	0.82	0.90

[a] Units = debye/PVF_2 repeat unit. [b] From ref 4. [c] Calculated from chain geometry.

The smallest net dipole is predicted for epitaxial films of the TGTG′ conformation, since two of the low-energy orientations have nearly antiparallel dipole moment orientations that cancel. For the T_2 conformation, the normal components of the dipole moment vector are parallel for the two low-energy orientations, but their sum represents only 17% of the total possible dipole moment (see column 3 of Table II). A similar situation exists for the T_3GT_3G' conformation, but in this case the normal components are larger and the net dipole moment expected for an epitaxial film composed of this conformation is actually larger than that of the T_2 conformation. However, the interaction energies indicate that T_3GT_3G' conformation is the least likely of the three to exist in epitaxial films on (111) CaF_2.

Conclusions

Single-chain interaction energy calculations for the three PVF_2 chain conformations predict that the all-trans conformation is strongly favored to deposit epitaxially on a CaF_2 (111) surface. The orientation of the polymer in the global energy minimum is such that a small net dipole remains in the epitaxial film (approximately 0.36 D/PVF_2 repeat unit). A larger net dipole is predicted for epitaxial films of the T_3GT_3G' conformation (0.90 D/PVF_2 repeat unit), even though this conformation was the least favored energetically to epitaxially deposit. The coulombic contribution to the total interaction energy is relatively high (30–48%) for all three conformations. Although polymer–polymer interactions and crystallinity effects are not included in these calculations, single-chain calculations such as these have been successful in predicting the orientation of epitaxially crystallized polymers.

Acknowledgment. We thank the Westinghouse Electric Corp., Measurements and Control Division, for the use of its computing facilities and the assistance rendered by members of its Product Software Engineering Group.

References and Notes

(1) Balik, C. M. *Macromolecules* **1986**, *19*, 1968.
(2) Bachmann, M.; Gordon, W. L.; Weinhold, S.; Lando, J. B. *J. Appl. Phys.* **1980**, *51*, 5095.
(3) Weinhold, S.; Litt, M. H.; Lando, J. B. *Macromolecules* **1980**, *13*, 1178.
(4) Sessler, G. M. *J. Acoust. Soc. Am.* **1981**, *70*, 1596.

Registry No. PVF_2, 24937-79-9; CaF_2, 7789-75-5.